

Controlling the ellipticity of attosecond pulses generated in the non-mirror regime of laser-plasma interaction

M. Blanco,¹ M.T. Flores-Arias,¹ and A. Gonoskov^{2,3,4}

¹*Photonics4Life reseach group, Departamento de Física Aplicada, Facultade de Física, Campus Vida, Universidade de Santiago de Compostela, 15782 Santiago de Compostela, Spain*

²*Department of Physics, Chalmers University of Technology, SE-41296 Gothenburg, Sweden*

³*Institute of Applied Physics, Russian Academy of Sciences, Nizhny Novgorod 603950, Russia*

⁴*Lobachevsky State University of Nizhny Novgorod, Nizhny Novgorod 603950, Russia*

(Dated: May 27, 2022)

The interaction of high-intensity laser pulses and solid targets provides a promising way to create compact, tunable and bright XUV attosecond sources that can become a unique tool for a variety of applications. However, it is important to control the polarization state of this XUV radiation, and to do so in the most efficient regime of generation. Using the relativistic electronic spring (RES) model and particle-in-cell (PIC) simulations, we show that the polarization state of the generated attosecond pulses can be tuned in a wide range of parameters by adjusting the polarization and angle of incidence of the laser radiation. In particular, we demonstrate the possibility of producing circularly polarized attosecond pulses in a wide variety of setups.

The generation of attosecond pulses during the ionization of noble gases by intense laser pulses [1, 2] has opened up wide opportunities for studying matter at previously unreachable attosecond time scales based on pump-probe metrology [3]. In these studies the attosecond pulses are mostly used as probes. The interaction of relativistically strong laser radiation with overdense plasmas provides a promising alternative for producing attosecond pulses of sufficiently high intensity that they can also be used as pumps. This can provide a principle tool for XUV-pump-XUV-probe metrology [4]. Controlling the polarization state of the generated attosecond pulses is interesting for these and other applications [5–9]. Such control has been recently demonstrated in simulations using overdense plasmas, which showed that by varying the interaction parameters it is possible to tune the polarization of the harmonics from linear to almost circular [10, 11]. Similar results have been also obtained for gas targets [12–14]. However, in the case of overdense targets, the relatively high values of plasma density considered in these studies correspond to the regime of the relativistic oscillating mirror (ROM) [15–17], which is significantly less efficient than the regime of the relativistic electronic spring (RES) [18]. The RES regime does not assume the limit of high density or the steep density profile that the ROM regime does, and therefore can be accessed with a realistic pre-plasma induced by finite laser contrast [19].

In this paper, we demonstrate how to control the ellipticity of attosecond pulses in a wide range of parameters related to the RES regime, in particular for the production of circularly polarized attosecond pulses. Moreover, we show that RES theory [20] perfectly describes the polarization properties of the generated attosecond pulse train for arbitrary polarization and angle of incidence of the laser pulse. By choosing the interaction parameters accordingly, one can therefore produce XUV pulses of

any preassigned ellipticity.

High-order harmonic generation (HHG) from the surface of an overdense plasma irradiated by a relativistically strong laser pulse has been especially well analysed under the assumption of steep density profiles and high plasma densities characterized by $S > 10$. Here $S = n/a$ is the similarity parameter, with n the plasma density in critical density units and a the radiation amplitude in relativistic units. In this case, the interaction can be well described by the ROM model [15–17, 21–24], which phenomenologically assumes equating the electromagnetic fluxes of the incoming and outgoing signals at some point oscillating around the plasma surface.

With decrease of the S parameter (i.e. increase of intensity and/or decrease of density) starting from $S \sim 10$ and until the emergence of relativistic self-induced transparency (RSIT) at $S \gtrsim 1/20$, the radiation propagation is still halted. However instead of repelling energy instantaneously, the plasma within each cycle first accumulates up to 60% of the incident energy and only then re-emits it back, acting as a spring [18]. The energy is stored in the form of electromagnetic fields, which arise when the radiation grabs and shifts inward frontier electrons relative to less mobile ions. In these situations, the shifted electrons tend to form a thin sheet, which moves so that its emission compensates the incident radiation in the plasma bulk. It is this phenomenological principle that underlies the RES theory [18, 20]. As the RES based theoretical model describes and provides insight into the variety of interaction scenarios, this regime can be referred to as the RES regime. A notable prediction is the generation of attosecond bursts with amplitude several times higher than the incident radiation [18, 25, 26]. The generation mechanism includes three stages: (1) energy accumulation due to the shift of the frontier electrons, (2) transferring the accumulated and incident energy to the thin sheet of electrons during its backward motion

and (3) emission of the burst by the sheet driven and energetically fed in this way. The last stage is also referred as coherent synchrotron emission (CSE) [27] and has also been studied in the case of laser interaction with a thin foil [28, 29].

Although the RES principle is valid for arbitrary incident polarization, all previous studies of this process have been done for the case of oblique incidence of P-polarized laser radiation, which naturally leads to linear polarization of the generated attosecond bursts. To analyze the effect of polarization we consider the problem using a rectangular coordinate system in a reference frame [30] moving along the plasma surface so that instead of oblique incidence we have normal incidence (towards the positive x direction) onto plasma streaming towards the negative y direction.

In the case of P-polarization, the electric field vector of the incident radiation is oriented along the y axis just as it is for the radiation that corresponds to the flow of uncompensated ions (in the region from which the electrons have been evacuated). Thus, in order to compensate the radiation in the plasma bulk the electrons in the sheet, apart from shifting in the x direction, should move only along the y direction, producing radiation with only non-zero y component of the electric field towards both positive and negative x . The former provides the compensation, while the latter appears as the generated linearly polarized attosecond bursts. Note that in this case the Lorentz force does not accelerate electrons in z direction (this kind of consistency of the RES principle with first principles has also been shown in [31]).

In the case of arbitrary polarization, to compensate the z component of the electric field of the incident radiation, the sheet has to move in the z direction as well. If both the y and z components of the sheet's velocity pass simultaneously through the vicinity of zero, the sheet moves with speed close to the speed of light in the negative x direction, emitting a short burst with singularly strong y and z electric field components. The ellipticity of the high-harmonics in this process arises from the asymmetry of passing the vicinity of the zero point and depends on the interaction parameters in a complex way.

To study the generation of ultrashort pulses with complex polarization states in the RES regime, we first verified the agreement between PIC simulations and the calculations for the RES theory with account for the motion of the electrons in z direction [20]. PIC simulations were performed using the code PICADOR [32, 33]. To simulate oblique incidence for an angle θ , we have used the boosted frame method, that consists in making a Lorentz transformation with a velocity of $c \sin \theta$ [30]. The PIC simulations were performed with a plasma having a steep density profile and consisting of electrons and heavy ions, with an initial density of $n = 360n_c$, where $n_c = \frac{m\omega^2}{4\pi e^2}$ is the critical plasma density, ω is the laser frequency and m and e are the mass and charge of the electron, respec-

tively. This plasma interacts with a laser pulse with a given polarization state and an amplitude of $a = 190$, given in relativistic units. The pulse has a rectangular profile with a duration of 6 laser periods.

Figure 1 displays the electron density (a), the incident field (b) and the reflected field (c) for a circularly polarized pulse with an angle of incidence of 45° . It demonstrates a perfect agreement between PIC simulations and the RES model numerical solver.

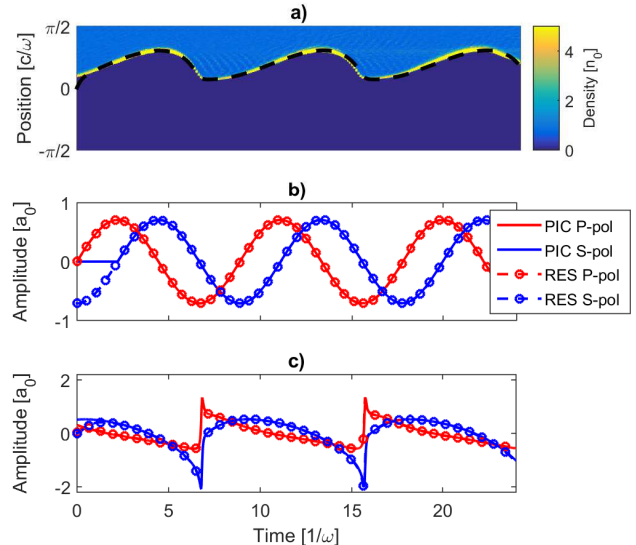


FIG. 1. (a) Electron density, (b) incident field and (c) reflected field for a circularly polarized pulse with an angle of incidence of 45° . The black dotted line on top of the electron density displays the thin sheet position calculated by the RES theory [20].

The agreement shown in figure 1 has been verified also in different configurations. The small mismatch present at the times near $t = 0$ happens because in our PIC simulations we initialize one of the field components after the other (according to their input phase difference), which is done to avoid nonphysical jumps in the incident field, while the RES solver calculates a periodic solution.

We have verified that RES calculations reproduce PIC results for arbitrary input polarization states and angles of incidence, hence we can use the RES theory to perform a parametric study to find the configurations that produce circularly polarized attosecond pulses. In our calculations we filter the harmonic orders $\omega \in [30, 60]$. To determine the polarization state of the generated burst, we calculate: (1) the ratio between the peak amplitudes corresponding to the minor (m) and major (M) components; (2) the phase difference between them. We assume that a pulse is circularly polarized when the ratio between its components is higher than 0.9 and the phase difference is in the ranges $\phi \in [80^\circ, 100^\circ]$ or $\phi \in [260^\circ, 280^\circ]$.

In the following analysis the laser intensity and the plasma density are fixed. We vary the angle of incidence

(θ), the ratio between the two polarization components of the laser radiation, and the phase difference (ϕ) between them. The parameter space spans angles of incidence θ between $[0^\circ, 60^\circ]$, phase differences ϕ between $[0^\circ, 90^\circ]$ and ratios for the component amplitudes between $[0, 1]$. We also consider two cases where the major axis corresponds to S-Polarization and P-Polarization. We have also verified that, as long as the parameters are in the applicability region of the RES model ($S < 10$, $a \gg 1$), the results are almost the same for different values of n and a that correspond to the same relativistic similarity parameter S .

Figure 2 shows 2D maps of the output ratio between minor and major axis (left column) and of the phase difference between them (right column), containing contours for the parameters associated with circular polarization. The input parameters for each of the cases shown in the figure have been chosen arbitrarily, in order to illustrate that the generation of circularly polarized pulses occurs for a wide range of parameters.

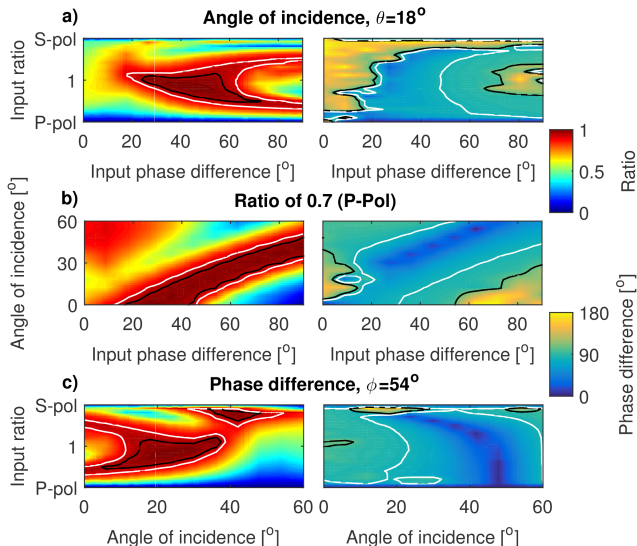


FIG. 2. Ratio (left column) and phase difference (right column) between minor and major axis for the filtered pulses. Results are shown for three examples of input parameters: (a) an angle of incidence of 18° , (b) a ratio between components of 0.7 (with the major axis P-polarized) and (c) a phase difference of 54° . Contours indicate ratios of 0.9 (white) and 0.95 (black) in the left column, while in the right column they indicate a phase difference of 80° (white) and 100° (black). The phase difference has been normalized to 180° .

Figure 2 shows that there are regions in the parameter space for which circularly polarized pulses are generated. This can also be seen from the figure 3, which shows isosurfaces for the ratio between the pulse components and phase difference, as well as the 3D parameter region in which circular pulses are obtained.

It is also interesting to notice from figure 3 that in-

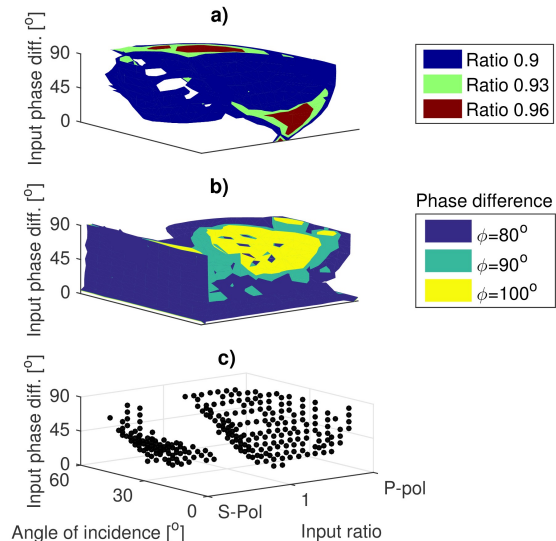


FIG. 3. Isosurfaces for the (a) ratio and (b) phase difference between minor and major axis. The bottom panel (c) shows the positions in the parameter space where circular ultrashort pulses are generated, which represent the intersection of the surfaces (a) and (b).

put pulses with linear or near linear S-polarization, can produce circularly polarized pulses, which does not happen for P-polarization. This satisfies the selection rules for HHG [16], which state that a S-polarized linear pulse in oblique incidence produces harmonics in the S- and P-polarization axes, while the same is not true for an incident P-polarized linear pulse.

Circularly polarized pulses can be produced in a variety of input setups. However, the emitted amplitude varies across these configurations. The most intense circularly polarized pulse that we have found has an amplitude on each component of $\sim 0.3a$, which is higher than reported elsewhere [10, 11]. Figure 4 illustrates the pulse train for this case. It displays the spectral and temporal form of a pulse train for both the RES model calculations and PIC simulations, showing good agreement. The parameters used for this figure are: a ratio between components of 0.5, with the P-polarized axis as major axis, a phase difference of $\phi = 81^\circ$ and an angle of incidence of $\theta = 36^\circ$. This configuration yields to the most intense circular ultrashort pulses of amplitude $\sim 0.3a$, with a FWHM of ~ 40 as.

We can conclude that circularly polarized attosecond pulses can be generated in a set of feasible experimental setups. The generation of these pulses has been demonstrated with the RES model, in agreement with the results obtained from 1D PIC simulations, proving that very high intensities can be achieved for a set of optimal parameters. This constitutes a theoretical basis for future experiments, opening a way to obtain these kind of pulses with several experimental setups.

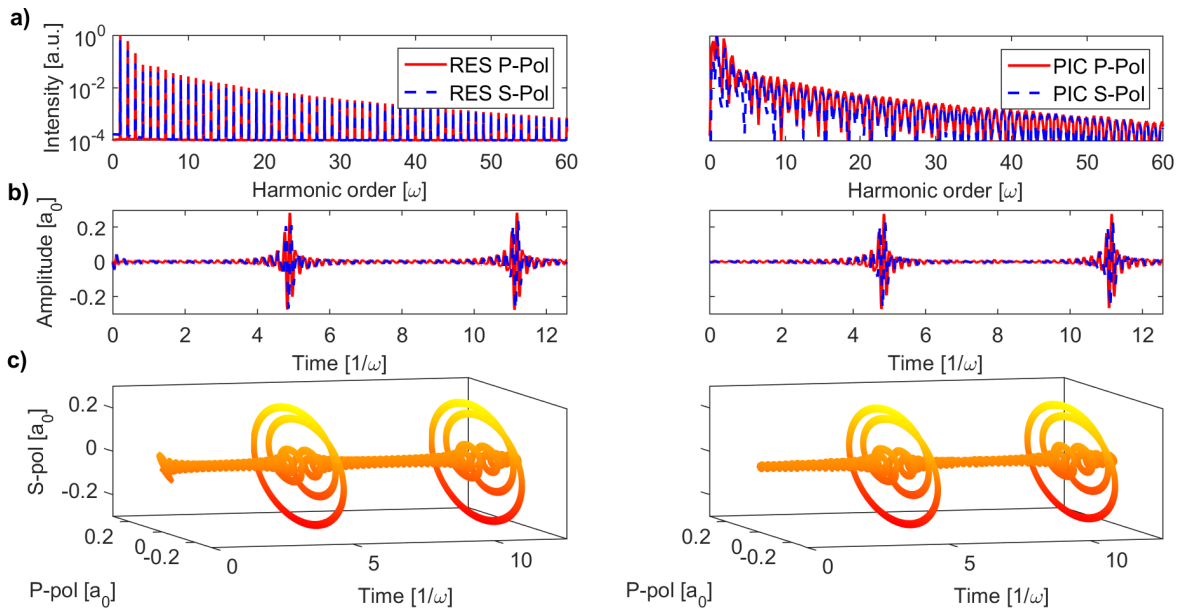


FIG. 4. Circularly polarized pulses obtained for the optimal parameters. The left column represents the result from RES calculations and the right column those from PIC simulations. In each row it is shown (a) the reflected spectral intensity for both polarization components, normalized to the fundamental harmonic order, (b) the temporal shape of the pulses obtained from filtering the harmonic orders between 30 and 60 and (c) a 3D view of these pulses, to better highlight their polarization state, respectively.

ACKNOWLEDGMENTS

This work has been partially funded by the Spanish Ministry of Economy and Competitivity (MINECO) under project MAT2015-71119-R, by Xunta de Galicia under project Agrup2015/11 (PC034), by the Knut and Alice Wallenberg project PLIONA and by the Swedish Research Council Grants No. 2012-5644 and No. 2013-4248. Manuel Blanco thanks the FPU grant program from the Spanish Ministry of Education, Culture and Sports (MECD). A. G. thanks T. G. Blackburn for useful discussions.

[1] P. Antoine, A. L’Huillier, and M. Lewenstein, *Phys. Rev. Lett.* **77**, 1234 (1996).
 [2] I. Christov, M. Murnane, and H. Kapteyn, *Phys. Rev. Lett.* **78**, 1251 (1997).
 [3] F. Krausz and M. I. Stockman, *Nat. Photon.* **8**, 205 (2014).
 [4] P. Tzallas, E. Skantzakis, L. A. A. Nikolopoulos, G. D. Tsakiris, and D. Charalambidis, *Nat. Phys.* **7**, 781 (2011).
 [5] S.-Y. Xu *et al.*, *Nat. Phys.* **8**, 616 (2012).
 [6] I. Gierz, M. Lindroos, H. Höchst, C. R. Ast, and K. Kern, *Nano Lett.* **12**, 3900 (2012).
 [7] G. Schütz, M. Knülle, and H. Ebert, *Phys. Scripta* **49**, 302 (1993).
 [8] T. Fan *et al.*, *Proc. Natl. Acad. Sci.* **112**, 14206 (2015).

[9] Y. Liu, G. Bian, T. Miller, and T.-C. Chiang, *Phys. Rev. Lett.* **107**, 166803 (2011).
 [10] Z.-Y. Chen and A. Pukhov, *Nat. Comm.* **7**, 12515 (2016).
 [11] G. Ma, W. Yu, M. Y. Yu, B. Shen, and L. Veisz, *Opt. Express* **24**, 10057 (2016).
 [12] D. B. Milošević and W. Becker, *Phys. Rev. A* **62**, 011403 (2000).
 [13] D. D. Hickstein, F. J. Dollar, P. Grychtol, J. L. Ellis, R. Knut, C. Hernández-García, D. Zusin, C. Gentry, J. M. Shaw, T. Fan, K. M. Dorney, A. Becker, A. Jaro-Becker, H. C. Kapteyn, M. M. Murnane, and C. G. Durfee, *Nat. Photon.* **9**, 743 (2015).
 [14] C. Hernández-García, C. G. Durfee, D. D. Hickstein, T. Popmintchev, A. Meier, M. M. Murnane, H. C. Kapteyn, I. J. Sola, A. Jaron-Becker, and A. Becker, *Phys. Rev. A* **93**, 043855 (2016).
 [15] S. V. Bulanov, N. M. Naumova, and F. Pegoraro, *Phys. Plasmas* **1**, 745 (1994).
 [16] R. Lichters, J. MeyerterVehn, and A. Pukhov, *Phys. Plasmas* **3**, 3425 (1996).
 [17] U. Teubner and P. Gibbon, *Rev. Mod. Phys.* **81**, 445 (2009).
 [18] A. A. Gonoskov, A. V. Korzhimanov, A. V. Kim, M. Marklund, and A. M. Sergeev, *Phys. Rev. E* **84**, 046403 (2011).
 [19] T. G. Blackburn, A. A. Gonoskov, and M. Marklund, (2017), [arXiv:1701.07268](https://arxiv.org/abs/1701.07268).
 [20] A. Gonoskov, (2017), [arXiv:1708.05364](https://arxiv.org/abs/1708.05364).
 [21] T. Baeva, S. Gordienko, and A. Pukhov, *Phys. Rev. E* **74**, 046404 (2006).
 [22] A. S. Pirozhkov, S. V. Bulanov, T. Z. Esirkepov, M. Mori, A. Sagisaka, and H. Daido, *Phys. Plasmas* **13**, 013107 (2006).

- [23] A. Debayle, J. Sanz, L. Gremillet, and K. Mima, *Phys. Plasmas* **20**, 053107 (2013).
- [24] T. Boyd and R. Ondarza-Rovira, *Phys. Lett. A* **380**, 1368 (2016).
- [25] J. Fuchs, A. Gonoskov, M. Nakatsutsumi, W. Nazarov, F. Quéré, A. Sergeev, and X. Yan, *Eur. Phys. J. Spec. Top.* **223**, 1169 (2014).
- [26] A. Bashinov, A. Gonoskov, A. Kim, G. Mourou, and A. Sergeev, *Eur. Phys. J. Spec. Top.* **223**, 1105 (2014).
- [27] D. V. der Brgge and A. Pukhov, *Phys. Plasmas* **17**, 033110 (2010).
- [28] J. M. Mikhailova, M. V. Fedorov, N. Karpowicz, P. Gibbon, V. T. Platonenko, A. M. Zheltikov, and F. Krausz, *Phys. Rev. Lett.* **109**, 245005 (2012).
- [29] S. Bulanov, T. Esirkepov, M. Kando, S. Bulanov, S. Rykovanov, and F. Pegoraro, *Phys. Plasmas* **20** (2013), 10.1063/1.4848758.
- [30] A. Bourdier, *Phys. Fluids* **26**, 1804 (1983).
- [31] D. Serebryakov, E. Nerush, and I. Kostyukov, *Phys. Plasmas* **22** (2015), 10.1063/1.4938206.
- [32] S. Bastrakov, R. Donchenko, A. Gonoskov, E. Efimenko, A. Malyshev, M. I., and I. Surmin, *J. Comput. Sci.* **3**, 474 (2012).
- [33] I. Surmin, S. Bastrakov, E. Efimenko, A. Gonoskov, A. Korzhimanov, and I. Meyerov, *Computer Physics Communications* **202**, 204 (2016).